

First-Principles Kinetics of CO Desorption from Oxygen Species on Carbonaceous Surface

Alejandro Montoya,[†] Fanor Mondragón,^{*,†} and Thanh N. Truong^{*,‡}

Institute of Chemistry, University of Antioquia, Medellín, Colombia, A.A 1226 and Henry Eyring Center for Theoretical Chemistry, Department of Chemistry, University of Utah, 315 South 1400 East, rm 2020, Salt Lake City, Utah 84112

Received: December 6, 2001; In Final Form: February 13, 2002

We present an ab initio direct dynamics study on the desorption of CO from semiquinone carbon–oxygen species in carbonaceous surfaces. Density functional theory, in particular B3LYP/6-31G(d) level, was used to calculate the potential energy surface information. We found that in the initial stage of the desorption process, the six-member ring of the carbonaceous model opens slightly to let the CO break away, and then closes up to form the five-member ring. Because of low-lying excited states in the carbon–oxygen complexes, electronic crossing occurs from reactants to products. Transition-state structures were found for the ground-state path, and the activation desorption energy is in excellent agreement with existing experimental data. Transition-state theory was used to calculate the thermal rate constant for desorption of CO in the range of 600–1700 °C. The fitted Arrhenius expression for the calculated rate constants is $k(T) = 1.81 \times 10^{17} \exp[-47682/T(\text{K})](\text{s}^{-1})$, which is within the experimental uncertainty for char gasification. In summary, we demonstrate that it is possible to model kinetics of elementary reactions in carbonaceous surfaces.

I. Introduction

Understanding the reactivity of carbonaceous surfaces in reactions with oxygenated agents has been the focus of many experimental studies because of its practical application in industry. In particular, kinetics evaluation of the char gasification has been a challenge issue because of the lack of detailed information on its mechanism. To improve the efficiency of the char gasification process, it is necessary to have knowledge of molecular-level detailed mechanisms of adsorption and desorption of different gases from the solid surface.

It has been suggested that desorption of CO can be the rate-determining step during the gasification of char under many conditions.^{1,2} Different complexes are responsible for the CO desorption, for instance, semiquinone, carbonyl, and ether. We differentiate the semiquinone group, >=O , that has the carbon atom of the C=O group as part of the six-member ring system from the carbonyl group, >=C=O , that has the carbon atom of the C=O group outside of the six-member ring. The existence of a distribution of intrinsically heterogeneous surface sites and broad spectra of surface oxygen complexes makes it difficult to measure experimentally kinetic parameters for CO desorption from a given surface oxygen complex. Thus, the relative importance of each complex in the overall CO desorption process remains unanswered. Quantum chemistry has appeared to be a viable alternative to provide insight into the CO desorption process. For instance, we have recently reported a density functional theory (DFT) study on the CO desorption from labile carbonyl surface oxygen complexes. We found that the desorption energies vary from 31 to 49 kcal/mol. This variation is due to the different local environments of the active sites as well as to the surface coverage of the char; the predicted desorption energies are in excellent agreement with TPD experimental data.³

Ether and semiquinone species are highly conjugated with the sp^2 -network of the carbonaceous surface, and CO desorption is expected to occur in the high-temperature regime. The stability of these carbon–oxygen complexes is greater than that of carbonyl groups and thus desorption activation energy would be higher. Therefore, desorption of CO from these oxygen complexes is important in the rate-controlling step in the mechanism of char gasification. Several authors have studied this reaction, that is, Skokova and Radovic have reported a semiempirical study of CO desorption from semiquinone carbon–oxygen complex and have found a CO desorption energy barrier of 64.7 kcal/mol.⁴ The authors used a coronene molecule as carbon model with no active sites. Chen and Yang have reported a combined nonlocal DFT/Hartree–Fock study of the CO desorption from semiquinone carbon–oxygen complexes; they found that the energy barrier for CO desorption estimated from the dissociation curves is about 156 kcal/mol.⁵ This is at least 76 kcal/mol higher than the experimental desorption activation energy at high temperatures.² The authors used a seven six-member ring model with several active sites. The previous works analyzed the effect of oxygen atoms on the basal carbon plane of the carbon model, and they found a decrease in the cleavage energy of the C–C bond next to the semiquinone group, which explains a decrease in the activation energy in the O_2 gasification in comparison with CO_2 and H_2O . However, CO desorption activation energy from semiquinone groups was not calculated. These works provided interesting insight but also raised several issues regarding the mechanism and kinetics of CO desorption process for oxygen species on char that require to be addressed in more details at an accurate level of theory.

In this study, we carried out a systematic study on the mechanism and kinetics of the desorption of CO from semiquinone carbon–oxygen complexes in carbonaceous surfaces from first principles. In particular, we paid close attention to different electronic states of the system as CO desorbs. This

* To whom correspondence should be addressed.

[†] University of Antioquia.

[‡] University of Utah.

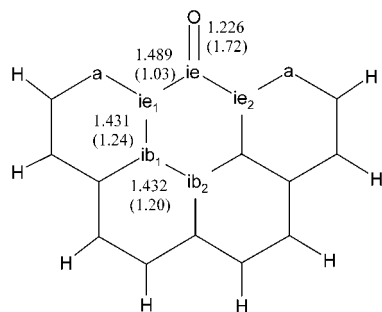


Figure 1. Semiquinone carbon–oxygen complex in the zigzag shape. Some carbon atoms are named to facilitate the discussion. a: active carbon atom; ie: inactive exposed carbon atom; ib: inactive buried carbon atom. Selected optimized bond length in Å. (x): Wiberg bond order.

aspect has not been examined previously. Kinetics of the desorption of CO is then calculated within the transition-state theory framework and the data are compared with existing experimental rate constants for CO desorption. Such a comparison allows us to draw conclusions on the accuracy and applicability of the computational modeling techniques, particularly for predicting kinetic and thermodynamic properties in the temperature range where experimental data are limited and for providing insight into the CO desorption process.

II. Computational Details

It is known from solid-state ^{13}C NMR experiments that char has structures of randomly connected graphene clusters consisting of 12–25 aromatic carbon atoms (3–7 benzene rings).⁶ Since an electron does not delocalize through single bonds efficiently, it is reasonable to assume that the reactivity of each graphene cluster is not affected by the remaining char structure. Active sites of char have been considered as unsaturated carbon atoms at the edge of the graphene layers.⁷ In support of the above assumption, our recent theoretical study showed that the reactivity of the active site depends mainly on its local shape rather than on the size of the graphene cluster;³ also Chen and Yang have shown that the reactivity of the carbon model does not depend strongly on the molecular size.⁸ Thus, in this study to model desorption of a CO molecule from a semiquinone carbon–oxygen complex, we used a five six-member ring in zigzag shape as shown in Figure 1. Two unsaturated carbon atoms at the edge of the carbon model were used to represent the active sites of the char as employed previously.⁸ Some carbon atoms are labeled to facilitate the discussion below, for instance, active carbons, a; inactive exposed carbons, ie; and inactive buried carbons, ib. Since physical models of char often contain several unsaturated carbon atoms to simulate the active sites, these unpaired electrons give rise to many low-lying excited states. Our primary goals are (1) to provide information on how different low-lying electronic states affect the energetics of the reaction as CO desorbs and (2) to examine the feasibility for predicting kinetics of this process from first principles. Previous modeling studies have proposed three different char configurations to model the active site, namely, zigzag, armchair, and tip shape.^{3,9} The use of only the zigzag shape model here is sufficient for our purpose. A complete study on the CO desorption from semiquinone surface species will be published in a separate report.

Electronic calculations were done at the B3LYP DFT level of theory, that is, Becke's hybrid three-parameter nonlocal exchange functional^{10–12} with Lee, Yang, and Parr's nonlocal correlation functional,¹³ using the 6-31G(d) basis set. This level

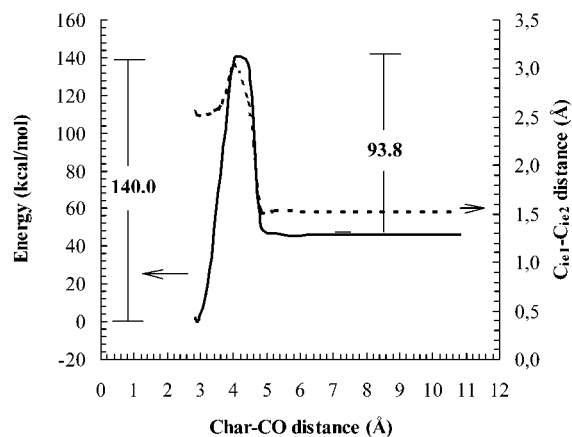


Figure 2. Triplet-state potential energy curve and optimized $\text{C}_{1e1}\text{--C}_{1e2}$ length at different char–CO distances, namely, the $\text{C}_{1b2}\text{--C}_{1e}$ distance.

of theory has been shown to provide accurate energetic properties of carbon–oxygen complexes in our previous studies.^{3,14} Unrestricted open-shell wave function was used in all open-shell cases. We have shown that the spin contamination in the unrestricted B3LYP is reasonably small and has acceptable small effects on the energetic properties of graphene layers.¹⁵ Electronic calculations were done using the GAUSSIAN 98 program.¹⁶ Thermal rate constant for the CO production was calculated at the transition-state theory (TST) using the Virtual Kinetic Laboratory.¹⁷

III. Results and Discussion

The semiquinone carbon–oxygen complex shown in Figure 1 was found to have two low-lying electronic states. The complex was fully optimized in its triplet ground state with a C_{2v} symmetry. The singlet excited state is only 0.1 kcal/mol higher. Selected optimized geometrical parameters and the Wiberg bond orders,¹⁸ which are related to the strength of the bonds, are shown in Figure 1. The $\text{C}_{1e}\text{--O}$ bond order of 1.72 suggests it is close to a double bond. Similarly, the $\text{C}_{1e1}\text{--C}_{1e}$ and $\text{C}_{1e2}\text{--C}_{1e}$ bonds are single bonds.

The desorption of the CO molecule is modeled by pulling the CO group away from the carbon model. To estimate the energy profile for this process, we calculated the potential curve as a function of the $\text{C}_{1b2}\text{--C}_{1e}$ distance starting from its ground-state equilibrium value to 11 Å at the interval of 0.3 Å while relaxing other degrees of freedom using the relaxed scan option provided by the Gaussian 98 program. Figure 2 shows the relaxed potential energy scan as a function of the $\text{C}_{1b2}\text{--C}_{1e}$ distance. The scan option uses the previously converged wave function as a guess for converging the SCF at the new point. Since we started the scan at the triplet ground-state equilibrium point, the potential scan maintains on the triplet surface. The $\text{C}_{1e1}\text{--C}_{1e2}$ distance was also plotted to show the mechanism for the ring closure upon desorption of CO. We found that in the initial stage of the desorption process, the ring opens slightly to let CO break away and then closes up to form the five-member ring. The variation of the $\text{C}_{1e1}\text{--C}_{1e2}$ distance along the desorption path resembles closely the potential curve plotted in the same figure. The CO desorption process proceeds with an energy barrier of about 140.0 kcal/mol, which is consistent with the previous theoretical study using a similar analysis.⁵ However, the previous study reported an unrelaxed scan at different theoretical levels of theory. In such scans, geometry was not allowed to relax as CO desorbs and thus ring closure was not observed. Ring closure stabilizes the product and gives

TABLE 1: Different Electronic Properties of the CO Desorption Structures at Different Char–CO Distances^a

$C_{ib2}-C_{ie}$ distance (Å)	2.931(ESC)	3.240	3.640	4.040	5.440
lowest electronic state	triplet	triplet	singlet	singlet	singlet
$\Delta E[GS-(CES)]$	0.1	0.4	0.1	37.9	1.5

^a $\Delta E[GS-(CES)]$: Energy difference (kcal/mol) between the ground State and the closest excited state. (ESC): equilibrium semiquinone complex.

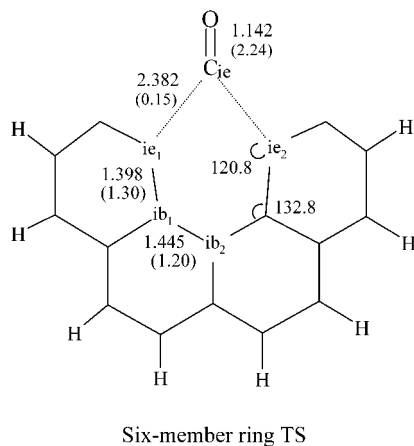


Figure 3. Singlet transition-state structure for the CO desorption from semiquinone surface complex. Selected optimized bond length in Å. (x): Wiberg bond order.

rise to the transition state as seen in Figure 2 where the backward reaction barrier for chemisorption of singlet CO is 93 kcal/mol. The experimental activation energy of the CO molecule desorption over 1000K is in the range of 79–92 kcal/mol,^{19,2} at least 48 kcal/mol lower than the calculated estimation from the potential energy scan. The B3LYP method is known to underestimate the barrier heights for many reactions by about 5–6 kcal/mol. Thus, the differences between theory and experiment are certainly too large.

To investigate the origin of such large differences, we carefully examined several electronic states of the equilibrium surface semiquinone complex at different points along the desorption pathway. The results are summarized in Table 1. First of all, the equilibrium semiquinone carbon–oxygen complex has a very low-lying singlet excited state that is only 0.1 kcal/mol above the triplet ground state. As CO desorbs in the direction that maintains the C_{2v} symmetry, that is, by breaking the two C–C bonds simultaneously, these two electronic states cross in the region where the $C_{ib2}-C_{ie}$ distance is between 3.64 and 4.04 Å. The lowest electronic state in the transition-state region and in the product channel is singlet. The difference between the lower singlet state and the triplet state is 37.9 kcal/mol, near the transition-state region which is close to the 48 kcal/mol overestimation in the barrier from the potential scan in Figure 2. To confirm this, the transition state was optimized in the singlet state. Selected geometrical parameters are given in Figure 3. In this six-member ring TS structure, the $C_{ie1}-C_{ie}$ bond order is 0.15, suggesting that a small interaction exists between the $C_{ie}-O$ group with the char surface. In particular, the bond $C_{ie1}-C_{ie}$ is 85% weaker and the $C_{ie}-O$ bond is 30% stronger than the same type of bonds in the semiquinone model. Normal-mode analysis shows that the transition state in fact corresponds to the CO desorption where the eigenvector of the imaginary frequency corresponds to distortion toward the semiquinone and the five-member ring product. As shown in Figure 4, the zero-point energy corrected barrier height was found to be 83.6 kcal/mol, which is consistent

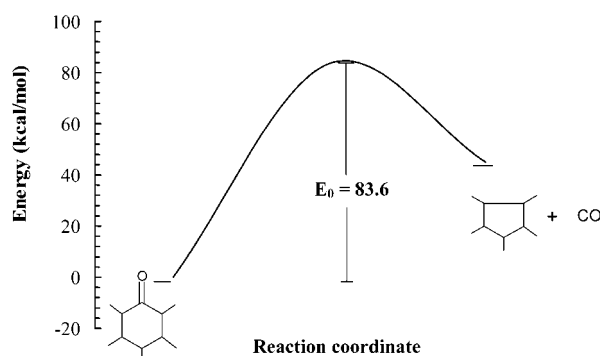


Figure 4. Schematic potential energy profiles for the singlet electronic state for the CO molecule desorption from a semiquinone surface oxygen complex. E_0 is the zero-point energy corrected barrier.

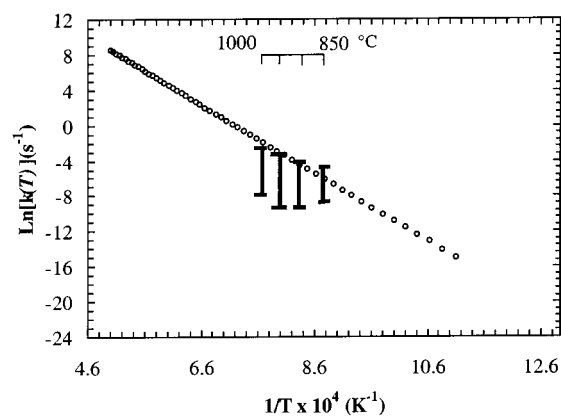


Figure 5. Comparison of the calculated and experimental rates $\text{Ln}[k(T)]$ versus $1/T(K)$. Bars are the experimental ranges obtained from the scientific literature.

with the experimental range. Thus, the origin of the large difference in the desorption energy found in Chen and Yang's previous study is mainly due to the surface crossing that was not modeled in the potential scan calculations.

Rate Constant. We have calculated thermal rate constants of CO desorption from the semiquinone carbon–oxygen complex in the temperature range from 600 to 1700 °C using the transition-state theory (TST). Vibrational partition functions were calculated quantum mechanically within the harmonic approximation while translational and rotational partition functions were computed classically. Both the triplet and singlet states were included in calculations of the reactant electronic partition function. The calculated forward rate constants were obtained for the singlet electronic state and are depicted in Figure 5 along with experimental data obtained from the scientific literature.^{1,2,20,21} Because experimental rate constants depend on the intrinsic reactivity of the carbonaceous solid and experimental conditions,²² the figure presents the range of the experimental rate constants obtained from temperature-programmed desorption for the CO release in the temperature range of 850–1000 °C of pure carbonaceous surfaces to avoid mineral matter effects. Experimental desorption rate constants shown in Figure 5 are based on the total CO desorption and do not differentiate between different surface complexes that desorb CO to the gas phase. However, since the desorption of CO from the semiquinone surface species is the rate-limiting step, one can expect their temperature-dependent rate constants to be similar to the total desorption rate. In fact, from Figure 5 the predicted rate constants for desorption of CO from the semiquinone complex are located within the experimental data. The difference between the experimental and calculated data be-

comes bigger at higher temperatures. Since semiquinone surface oxygen complexes are stable even at 950 °C,²⁰ the difference may be due to contributions from other more stable carbon–oxygen complexes, such as ether that affect the desorption process at higher temperatures. The fitted Arrhenius expression for the present calculated rate constants is $k(T) = 1.81 \times 10^{17} \exp[-47682\text{K}/T](\text{s}^{-1})$. From this expression, the activation energy is 94.8 kcal/mol, which is still within the experimental range. Since the rate constant for a specific surface complex has not been measured before, the calculated rate constants in the present work provide useful information for modeling desorption of CO from carbonaceous surfaces.

IV. Conclusions

We have performed a systematic study on the desorption of CO from oxygen species on carbonaceous surfaces from first principles. In particular, we found that because of the unpaired electrons located at unsaturated carbon atoms representing the active sites of char, the molecular system has several low-lying electronic states. As CO desorbs, these electronic states can cross. Careful examinations of such crossing allow us to correctly determine the potential energy profile for CO desorption from the semiquinone surface oxygen species. In addition, we obtained for the first time the temperature-dependent rate constant for this process using a model surface oxygen complex. The high CO desorption activation energy suggests that semiquinone complex has an important effect on the rate-limiting step on the char gasification mechanism. Our calculated rate constants are within the uncertainty of available experimental data indicating that the direct ab initio dynamics approach used in this study can be used to provide necessary thermodynamic and kinetic properties of important reactions in coal gasification process.

Acknowledgment. T. N. Truong acknowledges financial support from NSF and University of Utah. F. Mondragón and A. Montoya thank Colciencias and the University of Antioquia for financial support of the project No 1115-05-10853. A. Montoya thanks the seed grant given by the University of Utah.

We also thank the Utah Center for High Performance computing for computer time support.

References and Notes

- Huettinger, K. J.; Fritz, O. W. *Carbon* **1991**, *29*, 1113.
- Huettinger, K. J.; Nill, J. S. *Carbon* **1990**, *28*, 457.
- Montoya, A.; Truong, T.-T. T.; Mondragon, F.; Truong, T. N. *J. Phys. Chem. A* **2001**, *105*, 6757.
- Skokova, K.; Radovic, L. R. *Am. Chem. Soc., Div. Fuel Chem.* **1996**, *41* (1), 143.
- Chen, N.; Yang, R. T. *J. Phys. Chem. A* **1998**, *102*, 6348.
- Perry, S. T.; Hambly, E. M.; Fletcher, T. H.; Solum, M. S.; Pugmire, R. J. *Proc. Combust. Inst.* **2000**; Vol. 28, p 2313.
- Lee, C.; Walker, P. L., Jr.; Jenkins, R. G. *Fuel* **1983**, *62*, 849.
- Chen, N.; Yang, R. T. *Carbon* **1998**, *36*, 1061.
- Kyotani, T.; Leon y Leon, C. A.; Radovic, L. R. *AICHE J.* **1993**, *39*, 1178.
- Becke, A. D. *J. Chem. Phys.* **1992**, *97*, 9173.
- Becke, A. D. *J. Chem. Phys.* **1992**, *96*, 2155.
- Becke, A. D. *J. Chem. Phys.* **1993**, *98*, 5648.
- Lee, C.; Yang, W.; Parr, R. G. *Phys. Rev. B: Condens. Matter* **1988**, *37*, 785.
- Montoya, A.; Truong, T. N.; Sarofim, A. F. *J. Phys. Chem. A* **2000**, *104*, 8410.
- Montoya, A.; Truong, T. N.; Sarofim, A. F. *J. Phys. Chem. A* **2000**, *104*, 6108.
- Frisch, M. J.; Trucks, G. W.; Schlegel, H. B.; Scuseria, G. E.; Robb, M. A.; Cheeseman, J. R.; Zakrzewski, V. G.; Montgomery, J. A.; Stratmann, J. R. E.; Burant, J. C.; Dapprich, S.; Millam, J. M.; Daniels, A. D.; Kudin, K. N.; Strain, M. C.; Farkas, O.; Tomasi, J.; Barone, V.; Cossi, M.; Cammi, R.; Mennucci, B.; Pomelli, C.; Adamo, C.; Clifford, S.; Ochterski, J.; Petersson, G. A.; Ayala, P. Y.; Cui, Q.; Morokuma, K.; Malick, D. K.; Rabuck, A. D.; Raghavachari, K.; Foresman, J. B.; Cioslowski, J.; Ortiz, J. V.; Baboul, A. G.; Stefanov, B. B.; Liu, G.; Liashenko, A.; Piskorz, P.; Komaromi, I.; Gomperts, R.; Martin, R. L.; Fox, D. J.; Keith, T.; Al-Laham, M. A.; Peng, C. Y.; Nanayakkara, A.; Gonzalez, C.; Challacombe, M.; Gill, P. M. W.; Johnson, B.; Chen, W.; Wong, M. W.; Andres, J. L.; Gonzalez, C.; Head-Gordon, M.; Replogle, E. S.; Pople, J. A. *Gaussian 98*, Rev. A.9; Gaussian, Inc.: Pittsburgh, PA, 1998.
- Zhang, S.; Truong, T. N. VKLab, version 1.0. <http://vklab.hec.utah.edu> University of Utah, 2001.
- Wiberg, K. B. *Tetrahedron* **1968**, *24*, 1083.
- Ma, M. C.; Brown, T. C.; Haynes, B. S. *Surf. Sci.* **1993**, *297*, 312.
- Marchon, B.; Carrazza, J.; Heinemann, H.; Somorjai, G. A. *Carbon* **1988**, *26*, 507.
- Fritz, O. W.; Huettinger, K. J. *Carbon* **1993**, *31*, 923.
- Molina, A.; Mondragon, F. *Fuel* **1998**, *77*, 1831.